Journal of Alloys and Compounds 489 (2010) 162–166

Contents lists available at ScienceDirect

Journal of Alloys and Compounds

journal homepage: www.elsevier.com/locate/jallcom

High-frequency properties of Si-doped Z-type hexaferrites

Lijun Jia*, Jun Luo, Huaiwu Zhang, Gang Xue, Yulan Jing

State Key Laboratory of Electronic Thin Films and Integrated Devices, University of Electronic Science and Technology of China, Chengdu, 610054, PR China

ARTICLE INFO

Article history:
Received 30 July 2009
Received in revised form 31 August 2009
Accepted 1 September 2009
Available online 19 September 2009

Keywords:
Hexagonal ferrite
Sintering
Microstructure
Electromagnetic properties

ABSTRACT

In order to improve the high-frequency electromagnetic properties of $(Co_{0.4}Zn_{0.6})_2Z$ hexaferrites sintered at low-temperature, such as low magnetic loss tangent, low dielectric constant and loss tangent, SiO_2 was introduced. The effects of SiO_2 additive on the phase composition, microstructures and high-frequency electromagnetic properties of the ceramics prepared by a solid-state reaction method were investigated. The results from XRD show that in the doped samples the major phase, Z-type phase, coexists with a small amount of silicate phase. The grain growth of ceramics is suppressed by SiO_2 concentrated on grain boundaries and formed block stacking structure. As SiO_2 content increases, the static permeability and the dielectric constant continuously decrease. The samples with SiO_2 have lower magnetic loss tangent than that of the undoped sample. Meanwhile, all the samples with SiO_2 additive exhibit a low dielectric loss in the range of 400 MHz to 1 GHz. These materials are the excellent candidates to produce chip inductors for high-frequency use.

1. Introduction

With the development of communication and information technology, the electronic component with small size, high efficiency, and low cost are urgently demanded. The multilayer chip inductors (MLCI) have been rapidly developed as an important surface mounting device for electric applications. MLCI are fabricated by laminating the ferrite layers and the internal conductors alternately, and subsequently co-fired to form a monolithic structure. The key issue in MLCI manufacture is to realize the ferrite and internal electrode material layers that can be co-fired [1,2]. Considering the conducting and cost, silver is the most common used internal electrode material. Since the melting-point of silver is 961 °C, a sintering temperature around 900 °C is required for ferrites to avoid the diffusion of Ag in ferrites.

Up to now, NiCuZn spinel ferrites have been the dominant materials for MLCI due to its better magnetic properties at high-frequency and low sintering temperature [3,4]. However, it has limited operating frequencies below 300 MHz. As the trend of information technology electronic devices moves toward a high-frequency region, more attention has been paid to the planar Z-type hexagonal ferrite with composition of $Ba_3Me_2Fe_{24}O_{41}$ (Me: Co, Zn, Cu, Ni), which has a higher initial permeability, high thermal stability and a ferromagnetic resonance in the GHz region. This material is among the most widely used soft materials, instead of spinel ferrite, for high-frequency application, such as chip inductors, LC filters and microwave absorbers [5–8]. From the crystallographic point of view, Z-type hexaferrite is among the most complex compounds in the families of hexaferrites with planar hexagonal structure. Z-type hexaferrite can be treated as a sum of two simple hexaferrites, namely, of M-$(BaFe_{12}O_{19})$ and Y-$(Ba_2Me_2Fe_{12}O_{22})$ types. It is hard for Z-type phase to form directly from simple oxides. However, the sintering temperatures required to prepare pure Z-type hexaferrites via conventional solid-state reaction method are above 1200 °C. Various low melting-point sintering aids such as Bi_2O_3, CuO, WO_3 and PbO–CuO were usually introduced to decrease the sintering temperature [9,10]. The electromagnetic properties in high-frequency range of Z-type hexaferrite sintered at low-temperature were reported in our previous paper [11]. In order to improve its high-frequency performance (such as low magnetic loss tangent, low dielectric constant and loss tangent), SiO_2 which has a low dielectric constant was introduced into this system. In this paper, the effects of SiO_2 additive on the phase composition, densification, microstructures and electromagnetic properties of the hexaferrites were investigated.

2. Experimental procedure

Si-doped Z-type hexaferrites with composition of $Ba_3(Co_{0.4}Zn_{0.6})_2Fe_{23.6}O_{41}$ + $x$wt.%SiO_2 (x = 0–8.0) were prepared by a solid-state reaction method. The raw materials $BaCO_3$, α-Fe_2O_3, ZnO and Co_3O_4, of high purity, were mixed and calcined at 1270 °C for 2 h. Then the calcined powders were mixed with different amounts of SiO_2 additive and appropriate Bi_2O_3 additive (1.0–3.0 wt.%) and milled, dried and pressed. After secondary wet-milling, the ground powders were dried and added with 8.0 wt.% polyvinyl alcohol (PVA) solution for granulation and then pressed into the disc-shaped pellets (diameter 18 mm, thickness 1.5–3 mm) and toroidal samples (outside diameter 18 mm, inside diameter 8 mm, thickness 3–5 mm). All the bodies were heated to 600 °C with a ramping rate of 1.5 °C/min. The dwelling time at 600 °C

* Corresponding author. Tel.: +86 28 83201810 fax: +86 28 83201810.
E-mail address: jlj@uestc.edu.cn (L. Jia).

0925-8388/$ – see front matter © 2009 Elsevier B.V. All rights reserved.
doi:10.1016/j.jallcom.2009.09.043

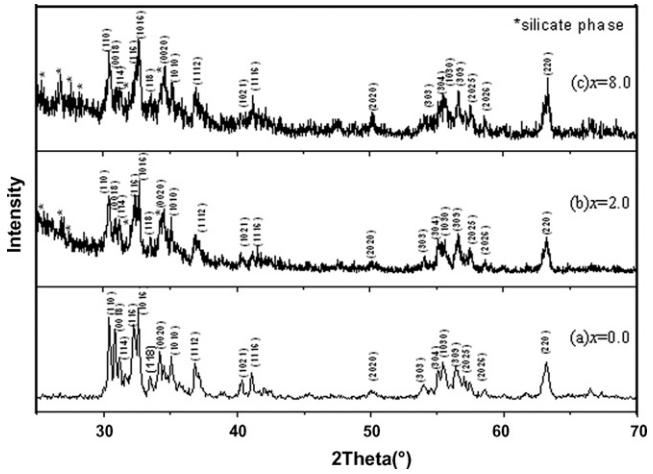

Fig. 1. XRD patterns of $Ba_3(Co_{0.4}Zn_{0.6})_2Fe_{23.6}O_{41}$ + x wt.%SiO_2 (x = 0, 2.0 and 8.0).

is 30 min to burn out the binders. The temperature was further increased to 900 °C with 2 °C/min ramping rate. Those bodies were sintered at 900 °C for 3 h in the air and then cooled in the furnace.

The structure of the samples was identified by means of X-ray diffraction (XRD: Philips X'Pert) using Cu Kα radiation in the range of 2θ = 25–70°. A scanning electron microscopy (SEM: S-4700) was used to observe the microstructure of the fracture surface of the samples. The bulk density was determined by the Archimedes method. The permeability spectrum and permittivity spectrum were measured by an HP4291B impedance analyzer. The permeability was measured on toroidal samples. The permittivity was measured on pellet samples by using conductive electrode. The direct current (DC) resistivity was measured by a TH4268 insulation resistance tester.

3. Results and discussion

The typical XRD patterns of Si-doped Z-type hexaferrites are shown in Fig. 1. It can be seen that all the samples are mainly of Z-type phase. As SiO_2 content increases, Z-phase coexists with a small amount of silicate phase. It is confirmed that some SiO_2 reacted with metal ions and formed the silicate phase ($BaZnSi_3O_8$) during sintering. The SEM images of Z-type hexaferrites with various amounts of SiO_2 additive (0, 0.5, 1.0 and 2.0 wt.%) are shown in Fig. 2. The undoped SiO_2 sample has a homogeneous hexagonal plate structure. The microstructures of all samples with SiO_2 are different from the undoped sample. With 0.5 wt.% SiO_2, the average grain size obviously decreases. Some grains are in an orderly arrangement. When x > 1.0, there are many large and small blocks formed with thin sheets in the samples. The crystal structure of Z-type hexagonal ferrite is complex and can be represented by a space group expression of $P6_3/mmc$. Its unit cell consists of 44 atomic layers which pile up to the c-axis. This structure may be described as a stack of six kinds of blocks, R, S, T, R^*, S^* and T^*, where R, S and T are independent and the asterisk indicates those 180°-rotated around the c-axis. The stacking order is $RSTSR^*S^*T^*S^*$. The crystallographic characteristics of Z-type hexaferrite determine that the shape of micron-sized hexaferrite particles calcined at high-temperature is anomalously flat. Among various diffusion routes, the grain boundary movement plays an important role for the densification and the recrystallization in the final sintering process. The element distribution was further analyzed by EDAX method (as seen in Fig. 3). The results show that Si element is concentrated on grain boundaries of hexaferrites. However, the average grain size decreases with increasing the doping content. It is suggested that the separated out secondary phase will restrain the movement of grain boundaries. Since the grain growth of hexaferrite in the direction of c-plane is dominant, the special block stacking microstructure can be formed due to SiO_2 concentrated on grain boundaries [12]. The bulk densities are 4.55 g/cm^3 for x = 0 wt.%, 4.03 g/cm^3 for x = 2.0 wt.% and 3.80 g/cm^3 for x = 8.0 wt.%. With increasing SiO_2 content, some secondary phase is separated out on grain boundaries, which leads to an increase of porosity on grain boundaries. Then the bulk density decreases slightly with the increase of SiO_2 content.

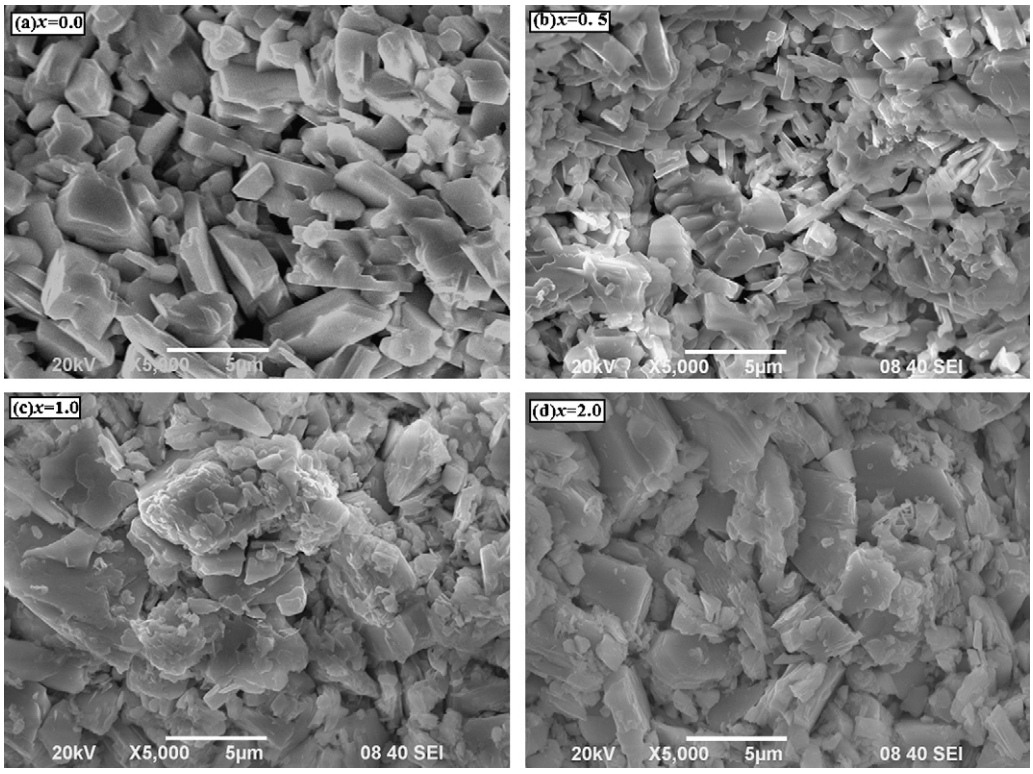

Fig. 2. SEM micrographs of the samples with different SiO_2 content (x = 0, 0.5, 1.0 and 2.0).

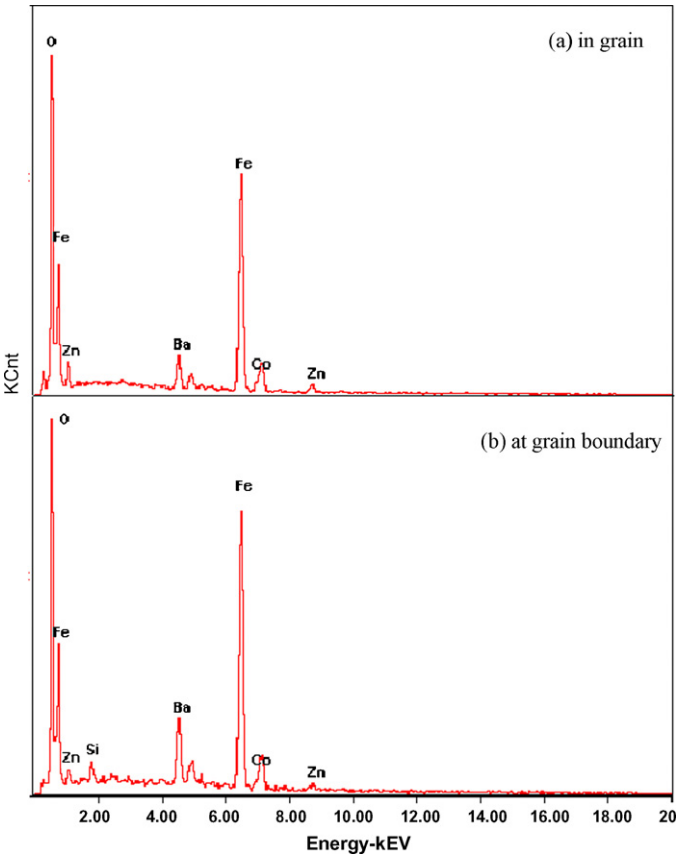

Fig. 3. EDAX microanalysis of $Ba_3(Co_{0.4}Zn_{0.6})_2Fe_{23.6}O_{41}$ + 2.0 wt.%SiO_2.

Fig. 4 shows the variation of DC resistivity (ρ) versus SiO_2 content for the low-temperature sintered samples. It is obvious that the resistivity values of all samples are greater than $10^8\ \Omega$ cm, and therefore meet the requirement of MLCI manufacturing. Furthermore, the DC resistivity continuously increases with SiO_2 content. This trend is attributed to the special structure of the ferrite, which is considered to consist of grains with higher conductivity and grain boundaries with lower conductivity. It is known that SiO_2 is concentrated in the inter-grain boundary of ferrites and provide the high electrical resistivity.

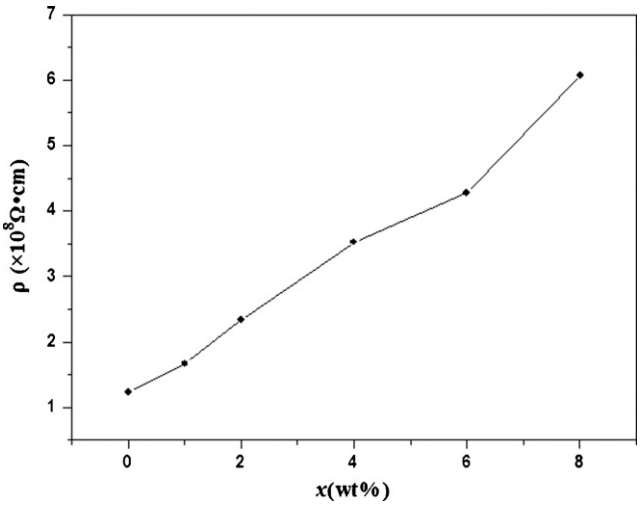

Fig. 4. Effect of SiO_2 content on the DC resistivity.

It is known that the magnetic domain structure and the thickness of the domain wall depend on the balance of various energies (magnetic anisotropy energy, stress energy, demagnetization energy, etc.) at the minimum. Obviously, the microstructures, including grain, grain boundary, porosity, secondary phase, etc., have an impact on the dynamic balance, as well as the static permeability. The variation of permeability of Z-type hexaferrites with SiO_2 content and frequency is shown in Fig. 5(a). It was found that the static permeability decreases with SiO_2 content. SiO_2 segregation at grain boundaries forms an insulating layer upon cooling [13]. In general, the magnetizing mechanism of soft ferrites is from domain rotation and domain walls motion. The domain rotation is closely connected to the sample density, and the domain walls motion is affected by the grain size and the sintering density [14]. The block stacking structure leads to a decrease of density and magnetic moment per unit volume. The decrease of density not only causes an increase of the demagnetizing field due to the existence of pores, but also reduces the spin rotation contribution, which in turn decreases the static permeability. With increasing the doping content, the existence of non-magnetic phase on grain boundaries pins the domain wall motion and cuts off the magnetic circuit, which leads to a decrease of static permeability. We can also see that the real permeability increases with the frequency approaching 1 GHz. This is attributed to the domain wall resonance and spin rotation relaxation. The SiO_2 grain boundary layer may act as a magnetic inactive layer as well as a high resistivity layer. The magnetic inactive layer causes the demagnetizing field and the cut of the magnetic connection between the magnetic components, and then the magnetic response to low magnetic field is suppressed. The magnetic susceptibility is decreased. The demagnetizing field generates an additional anisotropy field, that is, a shape anisotropy field. Subsequently, the effective anisotropy field is raised, since it is a vector summation of the crystalline anisotropy. Consequently, the static permeability decreases with an increase of the SiO_2 addition. In addition, the gap parameter δ/D (where δ is the distance between the ferrite particles, D is the average size of the ferrite particles) increases with the content of non-magnetic phase. Both the real and imaginary parts of permeability in the low-frequency region decrease when δ/D increases. These results coincide with the magnetic circuit model for ferrite composite materials [15]. As SiO_2 content increases, the magnetic loss tangent ($\tan\delta m$) decreases markedly. It is mainly caused by the magnetic inactive layer [16]. Since SiO_2 phase added in ferrite is mainly separated out on grain boundaries, the intergranular resistivity increases and the eddy current loss decreases with SiO_2 content.

As one of double-medium materials, Z-type hexaferrite possesses both magnetic and dielectric properties. When it is used in a circuit as an inductor, it will form an *LC* resonant circuit due to the effect of parasitic capacity. The resonant frequency (F_r) is described by the following equation:

$$F_r = 1/(2\pi\sqrt{LC}),$$

where L is the inductance and C is the capacitance. Consequently, in order to increase the application frequency range, the dielectric constant of the materials should be reduced to lower parasitical capacity and thereby to increase the resonant frequency. From Fig. 6(a) we can see that as SiO_2 content increases, the dielectric constant decreases to a certain degree. As a kind of polycrystalline ferrites, the resonance frequencies of electronic and ionic polarization of the samples appear beyond the frequency range of infrared. Considering that interfacial polarization always makes ε' reduce below 1 MHz, the dielectric properties vary in the range of 1 MHz to 1 GHz mainly due to the intrinsic electric dipole polarization, which is correlated with the electric domain structure, grain size and so on. Compared with the low-temperature sintered pure $(Co_{0.4}Zn_{0.6})_2Z$,

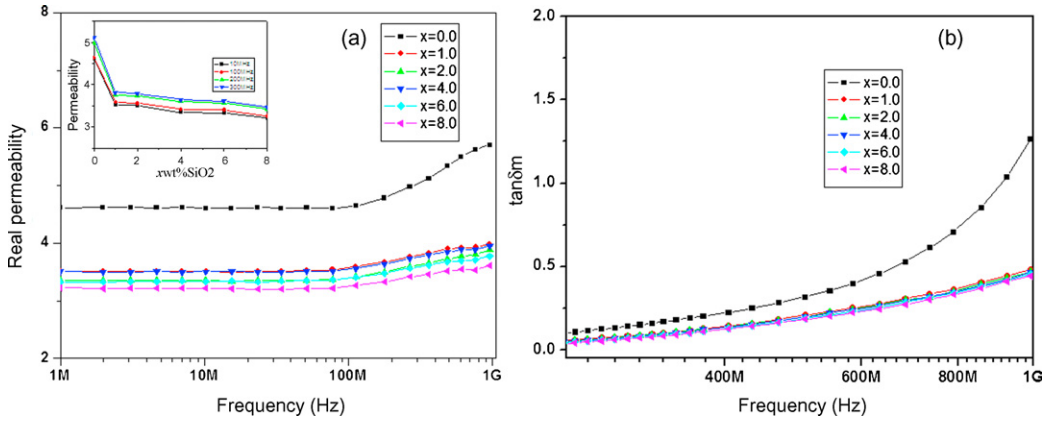

Fig. 5. Effect of SiO_2 content on the permeability (a) and the magnetic loss tangent (b).

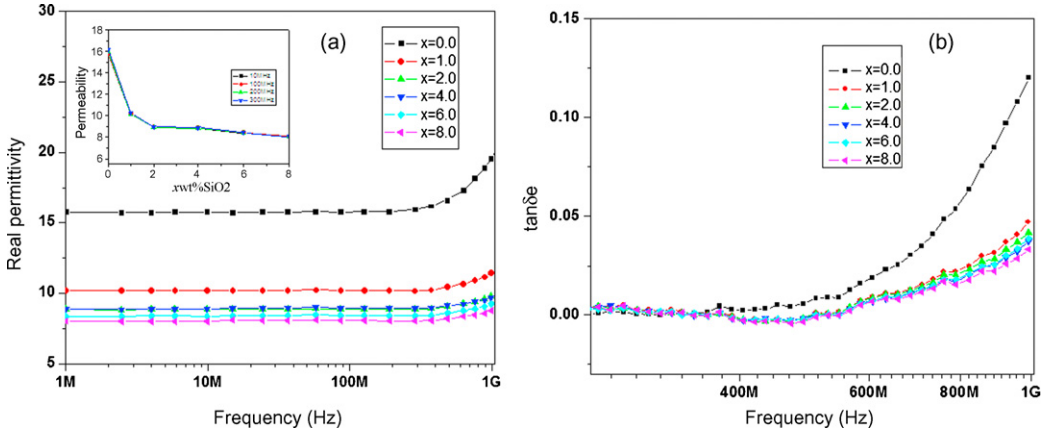

Fig. 6. Effect of SiO_2 content on the permittivity (a) and the dielectric loss tangent (b).

whose dielectric constant is about 16, the pure SiO_2 has a relatively low dielectric constant of about 6.0. As a result, the dielectric constant of the composition with SiO_2 additive should decrease as observed. We can also see that the real permittivity increases with the frequency approaching 1 GHz. This is attributed to the dielectric relaxation when the hopping frequency of electric charge carriers is applied AC electric field [17]. In addition, SiO_2 doping suppressed the grain growth, so that the proportion of the grain boundary was enhanced and this also contributed to the decrease of the dielectric constant. At the same time, the dielectric loss tangent ($\tan\delta e$) in the range of 400 MHz to GHz decreases with SiO_2 content. According to Kookps theory, the dielectric constant is directly proportional to the root mean square of the conductivity, or $\varepsilon^{\propto}(1/\rho^{1/2})$ [18]. The resistivity is enhanced by the increase of SiO_2 concentrations in grain boundaries. Furthermore, the grain size of the ferrites decreases with SiO_2 content as shown in Fig. 2. The proportion of the grain boundaries is assumed to be increased, thus resulting in an increase in DC resistivity.

4. Conclusion

In this work, in order to improve the high-frequency electromagnetic properties of Z-type hexaferrites, the effects of different SiO_2 content on the phase composition, microstructures and electromagnetic properties of hexaferrites were investigated. The modulation of SiO_2 additives on the electromagnetic properties of Z-type hexaferrites was discussed. SiO_2 grain boundary layer may act as a magnetic inactive layer as well as a high resistivity layer. As the amount of SiO_2 additive increases, the major phase, Z-phase, coexists with a small amount of silicate phase. With increasing SiO_2 content, the initial permeability and the magnetic loss tangent decrease. This could be mainly attributed to the non-magnetic phase which causes the cut of magnetic circuits, the increase in demagnetizing field and the decrease in grain size of hexaferrite. Meanwhile, the dielectric constant continuously decreases with SiO_2 content. And the loss tangent in the range of 400 MHz to 1 GHz evidently decreases by increasing the resistivity on grain boundaries. These materials are the excellent candidates to produce chip inductors for high-frequency use.

Acknowledgements

This work is partly supported by the Foundation for Innovative Research Groups of the NSFC under Grant no.60721001, the National found of China under Grant no.50872017, the International S&T Cooperation Program of China under Grant no. 2007/DFR10250.

References

[1] H. Sung, C. Chen, L. Wang, W. Ko, IEEE Trans. Magn. 34 (4) (1998) 1363–1365.
[2] Y. Wan, F. Chen, Y. Zhang, Electron. Comp. Device Appl. 5 (2003) 54–58.
[3] H. Su, H. Zhang, X. Tang, L. Jia, Q. Wen, Mater. Sci. Eng. B 129 (2006) 172–175.
[4] P.K. Roy, J. Bera, J. Magn. Magn. Mater. 298 (2006) 38–42.
[5] H. Zhang, L. Li, J. Zhou, J. Bao, Z. Yue, J. Mater. Sci.: Mater. Electron. 11 (2000) 619–622.
[6] Z.W. Li, G.Q. Lin, L.F. Chen, Y. Wu, C.K. Ong, J. Appl. Phys. 99 (2006) 063905.
[7] J. Jeong, K.W. Cho, D.W. Hahn, B.C. Moon, Y.H. Han, Mater. Lett. 59 (2005) 3959–3962.
[8] L. Jia, J. Luo, H. Zhang, Y. Jing, Y. Shi, Magn. Magn. Mater. 321 (2009) 77–80.
[9] H. Zhang, L. Li, Y. Wang, J. Zhou, Z. Yue, Z. Gui, J. Am. Ceram. 85 (2002) 1180–1184.

[10] Y. Mizuno, S. Taruta, K. Kitajima, J. Mater. Sci. 40 (1) (2005) 165–170.
[11] L. Jia, H. Zhang, Y. Liu, Z. Zhong, Q. Wen, J. Magn. Magn. Mater. 316 (2007) 67–72.
[12] L. Jia, S. Yin, H. Zhang, J.Q. Xiao, Q. Wen, J. Magn. Magn. Mater. 321 (2009) 1316–1320.
[13] N. Ramamanohar Reddy, M. Venkata Ramana, G. Rajitha, K.V. Sivakumar, V.R.K. Murthy, Curr. Appl. Phys. 9 (2009) 317–323.
[14] M. Arthur, J. Appl. Phys. 30 (4) (1959) S24.
[15] T. Nakamura, T. Tsutaoka, K. Hatakeyama, J. Magn. Magn. Mater. 138 (1994) 319–328.
[16] Y. Lin, S. Zhu, Z.R. Lin, Electron. Comp. Mater. 22 (2003) 37–40.
[17] A.M. Abo, E.I. Ata, M.A. El Hiti, J. Phys. III (France) 7 (1997) 883–894.
[18] C.G. Koops, Phys. Rev. 83 (1951) 121–124.